Proceedings of the XVIII ECSMGE 2024
GEOTECHNICAL ENGINEERING CHALLENGES
TO MEET CURRENT AND EMERGING NEEDS OF SOCIETY

ISBN 978-1-032-54816-6
DOI 10.1201/9781003431749-85

ECSMGE 24
XVIII EUROPEAN CONFERENCE ON SOIL MECHANICS AND GEOTECHNICAL ENGINEERING

A study on ultimate vertical bearing capacity of spread foundations of sand-clay two layers ground

Une étude sur la capacité portante verticale ultime des fondations étalées sur un sol à deux couches sablo-argileux

K. Kaneda*
Department of Civil Engineering, Chiba Institute of Technology, Narashino, Japan
S. Ohtsuka
Department of Civil and Environmental Engineering,Nagaoka University of Technology, Nagaoka, Japan
**kazuhiro.kaneda@p.chibakoudai.jp*

ABSTRACT: A rigid–plastic finite element analysis was used to study the bearing capacity of a two-layered ground consisting of sand and clay in the upper and lower layers, respectively. In general, a phenomenon in which a load propagating through a sand layer is distributed over a clay layer and applied to shear the clay layer is called distributed failure. Depending on the strength ratio of sand and clay, either the sand layer fails or distributed failure occurs in the clay layer. In addition, size effects occur when the foundation width increases in the sand layer. In this study, the ultimate bearing capacity of a spread foundation of two layers of sand and clay was examined using a higher-order function as a constitutive equation that considers the size effect. When the strength of the lower clay layer was relatively low, dispersion fractures were likely to occur.

RÉSUMÉ: L'analyse par éléments finis plastique rigide a été utilisée pour étudier la capacité portante d'un sol à deux couches constitué d'une couche de sable dans la couche supérieure et d'une couche inférieure dans la couche inférieure. En général, un phénomène dans lequel une charge se propage à travers une couche de sable, est répartie sur une couche d'argile et est appliquée pour cisailler la couche d'argile est appelé rupture distribuée. En fonction du rapport de résistance du sable et de l'argile, on considère que seule la couche de sable se brise ou qu'une rupture distribuée se produit dans la couche d'argile. De plus, des effets de taille sont connus lorsque la largeur des fondations augmente dans la couche de sable. Dans cette étude, la capacité portante ultime de la fondation étalée composée de deux couches de sable et d'argile a été examinée en utilisant une fonction d'ordre supérieur comme équation constitutive pouvant prendre en compte l'effet de taille. Il a été constaté que lorsque la résistance de la couche inférieure d'argile est relativement faible, une fracture par dispersion est susceptible de se produire.

Keywords: Ultimate vertical bearing capacity; RPFEM; size effect; two layered ground; distributed failure.

1 INTRODUCTION

Calculation of the ultimate bearing capacity of soil is important when designing a building (Terzaghi and Peck, 1967). The ultimate bearing capacity formulae for building foundations are specified in the guidelines published by the Architectural Institute of Japan (AIJ, 2019). These formulae are based on experimental and theoretical considerations of risk avoidance. However, the vertical bearing capacity of two-layered clayey soils has not been adequately investigated. Kaneda et al. (Kaneda et al., 2018) clarified the mechanism of bearing capacity considering squeeze breakdown of clayey soils. However, Kaneda et al. (Kaneda et al., 2018) investigated only clay grounds with two layers and did not consider cases in which the bottom layer was sand. In addition, when considering the vertical bearing capacity of spread foundations on sandy soil, the size effects must be considered. Nguyen Du et al. (Nguyen Du et al, 2016)explained the size effect by introducing a higher-order yield function using rigid plastic finite element method (RPFEM), which was developed separately by Tamura et al. (Tamura et al., 1984) and Asaoka and Ohtsuka (Asaoka and Ohtsuka, 1986). This method was employed to estimate the ultimate bearing capacity of the footings. The Drucker–Prager and high-order yield functions were adopted as the soil constitutive equations, and associated and non-associated flow rules were introduced to establish the configuration relationship of the ultimate state. Using this method, a structural safety assessment and calculation of the soil-bearing capacity were performed. In contrast to deformation

analysis, RPFEM is applicable to limited soil constants. It uses only strength parameters, such as cohesion and friction angle, since it addresses the limit state directly by disregarding the deformation of the building and ground. Since the RPFEM uses the upper-bound theorem of plastic theory, the end result is slightly larger than the true value. In this study, the vertical bearing capacities of two-layered clay and sandy soils were analyzed using numerical simulations.

2 BRIEF OUTLINE OF HIGH ORDER YIELD FUNCTION

The high-order yield function can be expressed as follows:

$$f(\boldsymbol{\sigma}) = aI_1 + (J_2)^n - b = 0 \tag{1}$$

where a, b, and n represent the material parameters. When n = 0.5, Eq. (1) corresponds to the Druker Prager model (DP model) function: assuming an associated flow rule, the strain rate and volumetric strain can be derived using Eqs. (2) and (3), respectively:

$$\dot{\boldsymbol{\varepsilon}} = \lambda \frac{\partial f(\boldsymbol{\sigma})}{\partial \boldsymbol{\sigma}} = \lambda \frac{\partial}{\partial \boldsymbol{\sigma}} \left(aI_1 + (J_2)^n - b \right) = \lambda \left(a\mathbf{I} + nJ_2^{n-1}\mathbf{s} \right) \tag{2}$$

$$\dot{\varepsilon}_v = tr\dot{\boldsymbol{\varepsilon}} = tr\left(\lambda \left(a\mathbf{I} + nJ_2^{n-1}\mathbf{s} \right) \right) = 3a\lambda = \frac{3a}{\sqrt{3a^2 + 2n^2 (b - aI_1)^{2-1/n}}} \dot{e} \tag{3}$$

where denotes the plastic multiplier. Based on Eqs. (1)–(3), the first stress invariant can be expressed as:

$$I_1 = \frac{b}{a} - \frac{1}{a} \left\{ \frac{1}{2n^2} \left[\left(3a \frac{\dot{e}}{\dot{\varepsilon}_v} \right)^2 - 3a^2 \right] \right\}^{\frac{n}{2n-1}} \tag{4}$$

Finally, the rigid plastic equation was calculated as follows:

$$\boldsymbol{\sigma} = \frac{1}{n} \left\{ \frac{9a^2}{2n^2} \left[\left(\frac{\dot{\mathbf{e}}}{\dot{\varepsilon}_v} \right)^2 - \frac{3a^2}{2n^2} \right] \right\}^{\frac{n}{2n-1}} \left[3a \frac{\dot{\boldsymbol{\varepsilon}}}{\dot{\varepsilon}_v} - a\mathbf{I} \right] + \frac{1}{3} \left[\frac{b}{a} - \frac{1}{a} \left\{ \frac{9a^2}{2n^2} \left(\frac{\dot{\mathbf{e}}}{\dot{\varepsilon}_v} \right)^2 - \frac{3a^2}{2n^2} \right\}^{\frac{n}{2n-1}} \right] \mathbf{I} \tag{5}$$

3 THEORETICAL DISTRIBUTED FAILURE

Regarding the vertical bearing capacity of the two-layered ground with a sand layer at the top and a clay layer at the bottom, the bearing capacity of the clay layer was evaluated by considering the load distribution by the sand layer. Figure 1 and Eq. (6) show the concept and evaluation formula for a distributed failure (Yamaguchi, 1963). If the foundation width (B) is larger than the sand layer thickness (H_s), the shear failure zone will reach the clay layer from the sand layer, and the shear resistance of the clay soil will affect the ultimate bearing capacity of the foundation considering the influence of ϕ. However, if $B<H_s$, shear failure occurs within the sand layer. Distributed failure is the phenomenon in which the load propagates through the sand layer and is distributed over the clay layer, causing shear failure of the clay layer.

$$q_{ac} = \frac{N_c B'}{F_b B} c + \gamma_t D + \frac{H_s p_o' K_0}{F_b B} \tan \phi' \tag{6}$$

where q_{ac} is bearing capacity of distributed failure (kPa), N_c is the bearing capacity coefficient, B is the foundation width (m), F_b is the safety factor, c is the cohesion (kPa), γ_t is the unit weight (kN/m^3), D is the penetration depth (m), and H_s is the upper sand layer thickness (m), p'_0 is the static coefficient, and K_0 is the earth pressure at rest, ϕ 'is the shear resistance angle of upper sand. $B'=B+2(H_s-D)\tan\alpha$. $p_0' = \gamma_t h_w + \gamma'(H_s - h_w)$ is the effective soil overburden pressure on the bottom surface of the sand. α is a dispersion angle.

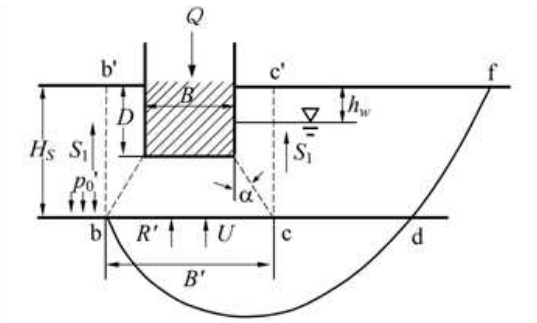

Figure 1. Distributed failure.

4 ANALYSIS CONDITIONS

Set B from 1m to 10 m; and set H_s to 0.5B, 1B, and 1.5B relative to foundation width B. Figure 2 shows the simulation mesh for a foundation width of 1 m and an upper sand layer of 1.5 m. The thickness and horizontal distance of the lower clay layer were set

such that a shear failure occurred within the simulation mesh, corresponding to the width of the foundation. The shear resistance angle ϕ was 30° and 40° for the upper sand layer, and the cohesion of lower clay layer was 20, 50, 100, and 150 kPa. The parameters of the higher order yield function were a=0.175, b=1.0, and n=0.526 for the ϕ 30° ground, and a=0.257, b=1.0, and n=0.526 for the ϕ 40° ground. The unit weight of the sand and clay layers was γ=18 kN/m^3, and the foundation rigidity was high. A vertical load was applied to the foundation to determine the ultimate vertical bearing capacity.

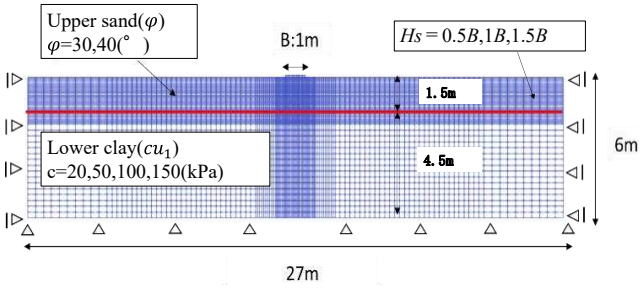

Figure 2. Simulation mesh (1m).

5 SIMULATION RESULTS

We investigated whether the simulation results were closer to a sand layer failure or distributed failure. The simulation results were organized by dividing them by the theoretical bearing capacity of sand layer failure and the theoretical bearing capacity of distributed failure (Eq. (6)). Note that the dispersion angle α in Figure 1 is 26.6° (1:2) and K_0 = 0.5. Figure 3 shows the relationship between the simulation results/sand layer failure (red), simulation results/distributed failure (blue), and the clay layer. The closer these values(the simulation results/sand layer failure or distributed failure) are to 1, the more it becomes clear whether the simulation result is a sand layer failure or a distributed failure. Also, ■ indicates the upper sand layer 0.5B, ▲ indicates 1B, and ● indicates 1.5B.

The focus was on the case where B=10 m. For ϕ =30°, if the strength of the lower clay layer is low, distributed failure is likely to occur, and if the strength of the lower clay layer is high, sand layer failure occurs. Figure 4 shows the shear strain distribution contours at failure at H_s = 1B (10 m) for the clay strength of (a) 50 kPa and (b) 150 kPa. Figure 4(a) shows a distributed failure including the lower clay layer, whereas form Figure 4(b), although there is some failure of the clay layer, most of the failure is of the sand layer. Next, considered ϕ =40°. Figure 5 shows the shear strain distribution contours at failure at H_s = 1B (10 m) with the clay strength of (a) 50 kPa and (b) 150 kPa. Figure 5(a) shows a distributed failure including the lower clay layer; however, a dispersion angle of 40° was more consistent with the analysis results than that of 26.6° from the appearance of shear failure. When calculating the theoretical value at the dispersion angle 40°, the simulated results/theoretical distributed failures were approximately 1.0. In contrast, in Case (b), a distributed fracture with a dispersion angle of 26.6° was observed.

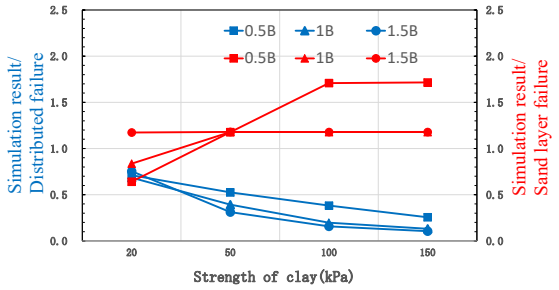

(a) B=1 m ϕ=30 ° (sand)

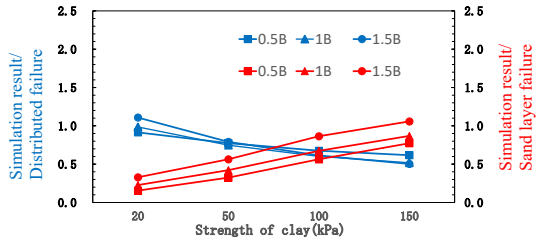

(b) B=1 m, ϕ=40 ° (sand)

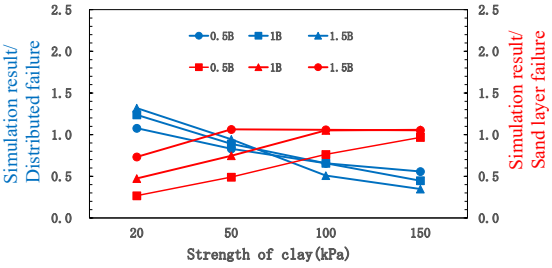

(c) B=10 m ϕ=30 ° (sand)

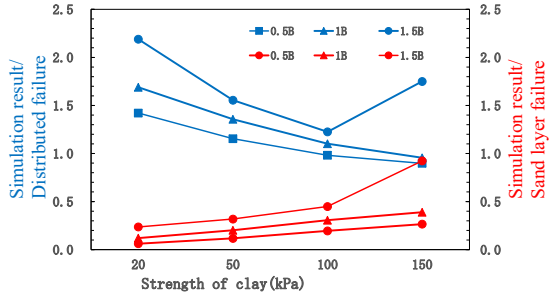

(d) B=10m, ϕ=40 ° (sand)

Figure 3. Relationship between the simulation result/sand layer failure (red), simulation result/ distributed failure (blue), and underlying clay layer.

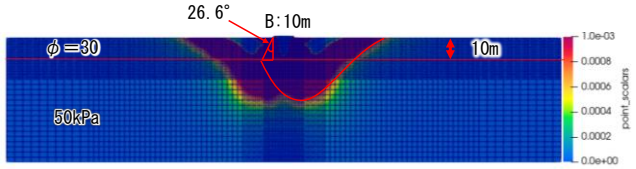

(a) Clay strength of 50 kPa

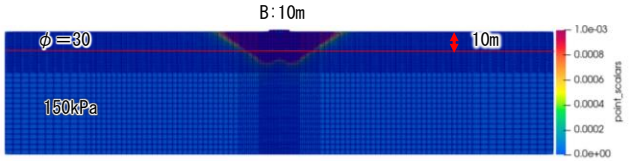

(b) Clay strength of 150 kPa

Figure 4. shear strain distribution contours at failure at H_s = 1B (10 m), ϕ=30 ° (sand).

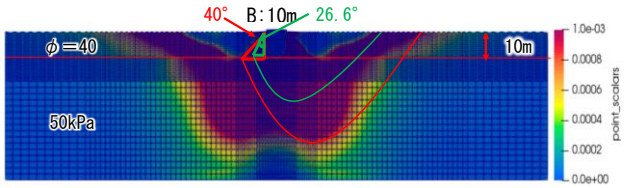

(a) Clay strength of 50 kPa

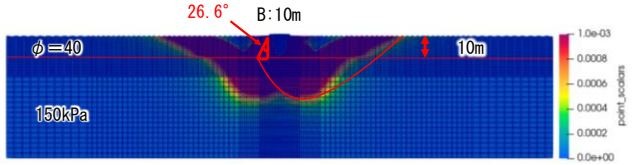

(b) Clay strength of 150 kPa

Figure 5. shear strain distribution contours at failure at H_s = 1B (10 m), ϕ=40 ° (sand).

6 CONCLUSIONS

The vertical bearing capacity of the two-layered soil was investigated using the RPFEM with higher-order yield functions.

For the strength of the upper sand layer of ϕ = 30° and a low strength of the lower clay layer, a distributed failure occurs, and conversely, for a high strength of the lower clay layer, a sand layer failure occurs. The dispersion angle is 26.6°.

For the strength of the upper sand layer of ϕ = 40°, a distributed failure occurs, and for the low strength of the lower clay layer, the dispersion angle is large, and conversely, for the high strength of the lower clay layer, the dispersion angle is 26.6°.

ACKNOWLEDGEMENTS

We would like to thank Takumi Araki, second year master's student at Chiba Institute of Technology for organizing these simulations.

REFERENCES

Architectural Institute of Japan (2019). AIJ. Recommendations for design of building foundation, pp. 112–136. (in Japanese).

Asaoka, A. and Ohtsuka, S. (1986). The analysis of failure of a normally consolidated clay foundation under embankment loading, Soils and Foundations, 26(2), pp. 47–59. https://doi.org/10.3208/sandf1972.26.2_47

Hakujyu Yamaguchi (1963). Practical formula of the bearing capacity for two layered ground, *Proceedings of 2nd ARCSM*, Vol. 1.

Kaneda, K., Aoki, M. and Ohtsuka, S. (2018). Ultimate bearing capacity of footing of two layered clayey soil system by rigid-plastic finite element method, *Proceedings of 8th International Conference on Geotechnique, Construction Materials and Environment, Kuala Lumpur, Malaysia*, Nov. 20-22, ISBN: 978-4-909106001 C3051.

Nguyen Du L., Ohtsuka S., Hoshina T. and Isobe K. (2016). Discussion on size effect of footing in ultimate bearing capacity of sandy soil using Rigid plastic finite element method, Soils and Foundations, Vol 56, No.1, pp. 93-103. https://doi.org/10.1016/j.sandf.2016.01.007

Tamura, T., Kobayashi, S., and Sumi, T. (1984). Limit analysis of soil structure by rigid plastic finite element method, Soils and Foundations, 24(1), pp. 34–42. https://doi.org/10.3208/sandf1972.24.34

Terzaghi, K. and Peck, R.B. (1967). Soil Mechanics in Engineering Practice, John Wiley & Sons, pp. 472–569.